Temperature stability of a pure metakaolin based K-geopolymer: Part 2. Variations in the mesoporous network and its rehydration stability

Sandrine Gomes, Elodie Petit, Lawrence Frézet, Jean-Marie Nedelec, Ameni Gharzouni, Sylvie Rossignol, Guillaume Renaudin

Temperature stability of a pure K-geopolymer: Part 2. Variations in the mesoporous network and its rehydration ability.

Sandrine GOMES,[1] Elodie PETIT,[1] Lawrence FREZET,[1] Jean-Marie NEDELEC,[1] Ameni GHARZOUNI,[2] Sylvie ROSSIGNOL,[2] Guillaume RENAUDIN[1]*

[1] Université Clermont Auvergne, CNRS, SIGMA Clermont, ICCF, F-63000 Clermont-Ferrand, France.

[2] IRCER, Université de Limoges UMR3571, 12 rue Atlantis, 87068 Limoges, France.

Abstract:

The thermal behavior of a model MK based K-geopolymer was investigated between room temperature and 1400 °C in order to evaluate its potentiality for high-temperature applications. The purpose of our study was to monitor the behavior of a geopolymer during a temperature rise in order to better understand its variations with respect to temperature. The works from the present paper focus only changes in the porous network; it follows a first part devoted to variations in the mineral matrix. The results obtained here show that the geopolymer material preserves its porous integrity up to 800 °C, while maintaining the reversibility of water exchanges corresponding to about 25 weight percent. Together with the results of part 1, the findings of this study allow us to affirm that geopolymer materials are only very little affected by temperatures up to 800 °C, or even 900 °C (keeping its mesoporous amorphous structure).

Keywords: Geopolymers; Characterization; Thermal treatment; Densification.

* Contact: Pr Guillaume Renaudin, guillaume.renaudin@sigma-clermont.fr

1- Introduction

Geopolymers, the usual name for the more conventional denomination of alkali aluminosilicate gels, are inorganic solids obtained by the alkaline activation of an aluminosilicate precursor. The precursor can be either a calcined clay (usually metakaolin, a dehydroxylated natural kaolin) or low-calcium aluminosilicate industrial by-products (fly ashes or ground blast furnace slag). In most cases these precursors are activated with an alkaline aqueous solution based on sodium or potassium, which induces the dissolution of the precursors followed by the polymerization of $[AlO_4]^{5-}$ and $[SiO_4]^{4-}$ tetrahedra into a three-dimensional network. The solid obtained is completely amorphous[1-4] and porous,[1,5,6] and presents interesting mechanical properties.[7,8] Geopolymers belong to the family of inorganic binders, however their setting mechanism and setting products – linked to the geopolymerization reaction[3,9-11] – are fundamentally different from the hydration process of conventional Portland cements. Geopolymer binders generate a significant improvement in CO_2 emissions (compare to Portland cement production),[12-15] present unusual thermal and acid resistance,[7,16-19] as well as the ability to stabilize various kinds of wastes (including nuclear wastes).[20-23] Geopolymers are characterized by high thermal stability, which makes them promising candidates for various applications. Many authors have investigated the thermal behavior of metakaolin-based geopolymers. For instance, Duxson et al.[24,25] studied the structural variations in sodium-based geopolymers at temperatures up to 1000 °C using DTA, quantitative XRD and FTIR. They found that phase stability is Si/Al ratio-dependent, with two different densification mechanisms: viscous flow and the collapse of the pore network. Both are responsible to a large extent for thermal shrinkage. It has been demonstrated that the beginning of the crystallization process, corresponding to the loss of the amorphous characteristic of the geopolymer, is also Si/Al ratio-dependent and alkaline dependent, with the formation of $(Na,K)AlSiO_4$ above 850°C.[24,26-28] In parallel with these physicochemical transformations, mechanical properties are

also affected by the temperature.[29] Despite the advanced research concerning the thermal behavior of metakaolin-based geopolymers, further fundamental knowledge is required in order to understand the chemical and structural variations in the geoplymer network as a function of the temperature, and therefore to evaluate their potential for high-temperature applications as refractories and in fire-retardant or fireproof applications.

In the first part of this study, the thermal stability of the mineral matrix of a potassium-based geopolymer was highlighted up to a temperature of 900 °C, before crystalizing into kalsilite and leucite.[30] In order to complete our investigations on the refractory potential of such a geopolymer, we are focusing in the present paper on the behavior of the porous part of the material when subjected to a temperature increase: the pore dimensions in volume and radius, and also its ability for rehydration. It is well accepted that the polycondensation of silicate and aluminate species, at the origin of the formation mechanism of geopolymers, enables a porous material to be obtained with an alkaline residual solution contained in the pores. Mercury intrusion and gas adsorption-desorption isotherm techniques are in favor of a monomodal open mesoporosity for geopolymers.[5,31-35] Nevertheless, direct observations made by transmission electronic microscopy are in favor of a poorly-defined – in size and in shape – porous network,[36] implying the notion of an "ink-bottle" effect. Other studies have also evidenced the presence of macroporosity in combination with the mesoporous network.[37-40] The purpose of our work is to determine not so much the fine characteristics of the porous network as its variations with temperature, always with the aim of probing the potential of geopolymers for high-temperature applications because the water contained in the pores, of the order of 25 weigh percent,[41] provides interesting fire-resistant properties.

The precise characterisation of both geopolymer sub-networks will then be decisive in understanding the fire-resistant properties of the material. Thus, our fundamental studies aim to help in the formulation of a thermally resistant geopolymer composition with the aim of

developing a mineral binder with fireproof properties. The targeted material could be used to protect nuclear waste containers and drifts for the planned construction of a geological disposal centre for radioactive waste (Cigeo project carried out by The National Agency for the Management of Radioactive Waste - Andra).

2- Materials and methods

2.1 geopolymer synthesis, thermal treatments and storage conditions

The samples used in this paper were exactly those previously prepared and characterized in Part 1 of this study.[30] As a summary, the geopolymer was obtained by the potassium silicate activation of a metakaolin of high purity – non-commercial product – supplied by Imerys (AGS quarrying, F-17270 Clérac, France). The samples were called T^{RH} with T the heat treatment temperature after geopolymer preparation (25, 100, 200, 300, 450, 600, 700, 800, 900, 1000, 1100, 1250 or 1400) and *RH* the storing conditions after heat treatment ('95' for 95 % RH, '30' for 30 % RH or 'bak' for the baked powders), making a total of 37 samples. The interest of these three series was to have different water filling levels for the porous network; from water-saturated (T^{95} series) to dry geopolymers (T^{bak} series), with an intermediate water filling level (T^{30} series). Figure S1 in the supplemental material superimposes the thirteen heat treatments used with a thermogravimetric analysis of the geopolymer.

2.2 ^{1}H solid-state NMR spectroscopy

^{1}H solid-state NMR experiments were performed using a 300 MHz Bruker spectrometer operating at 7.04 T, the Larmor frequency being 300.1 MHz. ^{1}H solid-state NMR experiments were carried out using MAS at 30 kHz and a 2.5 mm-diameter zirconia rotor. Static measurements were systematically performed. ^{1}H MAS spectra were recorded using one pulse

sequence and a recycling time of 5 s; chemical shifts were calibrated using adamantane at 1.7 ppm.

2.3 DSC measurements and TPM analyses

For thermoporosimetry (TPM) analyses, the water inside the geopolymer was chosen as a probe solvent. TPM analyses were performed by differential scanning calorimetry (DSC) measurements using a Mettler-Toledo DSC 823e apparatus, with STARe software. The DSC apparatus was calibrated (both for temperature and enthalpy) with metallic standards (In, Pb) and water. About 70 mg of the crushed geopolymer sample was introduced into an aluminium DSC crucible of 160 µl. The measurement procedure, under compressed air in airtight crucibles without adding external water, included the four following segments: cooling from room temperature to -60 °C at a rate of 10 °C/min; heating from -60 °C to -1 °C at a rate of 0.7 °C/min; renewed cooling from -1 °C to -60 °C at a rate of 0.7 °C/min; and finally heating to 25 °C at a rate of 10 °C/min to return to room temperature (Figure 1). This procedure enables the characterization of only the porous volume saturated with water under the different storage conditions. A slow rate of 0.7 °C/min was chosen to allow continuous thermal equilibrium inside the DSC cell. Crystallization curves (segment 3) were mainly used for calculation purposes, but corresponding events in the melting curve (segment 2) were systematically checked to avoid artefacts and to determine pore geometry. The calibration of water as a thermoporosimetric probe has been already published by Brun and co-workers.[42] The following empirical relationships were used:

$$R_p(nm) = -\frac{64.67}{\Delta T} + 0.57 \qquad \text{Equation 1}$$

$$W_a(Jg^{-1}) = -5.56.10^{-2}\Delta T^2 - 7.43\Delta T - 332 \qquad \text{Equation 2}$$

where ΔT is the shift of the thermal transition temperature, R_p the pore radius and W_a is the apparent energy of crystallization for water. The application of TPM formalism beyond the mesoporous domain has been already validated and applied on geopolymer samples,[41] but for the first time we used internal water to probe only the saturated porous volume.

2.4 Gas absorption isotherms

Nitrogen adsorption-desorption isotherms were obtained using a Micromeritics ASAP 2020 instrument at 77 K. The geopolymer degassing process was carried out under two vacuum stages at different temperatures depending on the temperature of the heat treatment applied to the geopolymers. The first step was performed under primary vacuum during at least 24 hours at room temperature for the as-synthesized geopolymer (25^{30} sample), 100 °C for the 100^{30} sample, and 200 °C for all the other T^{30} samples (with $T \geq 200$). Then a secondary vacuum was applied without modifying the temperature. The second degassing process was controlled by checking the back pressure increase rate after 5 min and 10 min of equilibration. This controlled back pressure was judged satisfactory for values below 10 µm Hg/min. The second degassing duration was sample-dependent to achieve this condition. The average pore size was calculated using the Barrett, Joyner and Halenda (BJH) method[43] and the specific area was determined using the Brunauer, Emmet and Teller (BET) theory.[44]

3- Results

3.1 ^{1}H NMR spectroscopy

3.1.1 ^{1}H NMR static spectra on samples stored at 95% RH

First, ^{1}H NMR static measurements were performed on samples stored at 95% RH in order to evidence the liquid nature of the water present in the geopolymer. As-prepared samples presented a well-defined signal with a single component close to 4.5 ppm, corresponding to

free water molecules located in the porous network. For heat-treated samples (stored at 95% RH) the same signal was still observed. This signal became finer when the temperature increased to 700 °C, then decreased in intensity toward 900 °C before disappearing at 1000 °C. Above 900 °C, the recorded signal corresponded to that of the rotor only (Figure 2a). These results clearly evidence the liquid nature of the water located in the pores of the geopolymer, its reversible departure indicating the open feature of the porous network. The modeling of these signals by a Lorentzian component indicated the sharpening of the signal without modification of its chemical shift (Figure 3b). The Full Width at Half Maximum (FWHM; Figure 3c) of this signal, centred at about 4.5 ppm, is divided by two between room temperature (FWHM = 5.0 ppm) and 600 °C (FWHM = 2.5 ppm), indicating an increase in the 'liquid nature' of the pore water – i.e. an increase in the water dynamic parameters – which could be due either to a decrease in its containment (increase in pore diameter), to a change in the nature of the interface (wall between the mineral and porous networks), or to a decrease in water salinity (i.e. decrease in its alkalinity).[45-53]

3.1.2 ^{1}H NMR MAS spectra for samples stored at 95% RH

The results from ^{1}H MAS NMR measurements were very close to the previous ones, again with a single Lorentzian component centered around 4.5 ppm (more precisely around 4.6 ppm for static measurements, slightly shifted to around 4.4 ppm for dynamic measurements; Figures 2b and 3b). The 30 MHz rotation speed enabled an increase in the 'aqueous nature' of the probed hydrogen atoms, leading to a general refinement of the signals, which still presented a decrease in their FWHM as the heat treatment temperature rose (from FWHM = 4.0 ppm at room temperature to FWHM = 1.0 ppm at 600 °C; Figure 3c). The same general trends observed simultaneously in static and dynamic measurements indicated that overall the hydrogen atoms from geopolymers belong exclusively to free water molecules located in the porous network.

Similar results have been observed for liquid water molecules filling the mesopores in silica glass.[54] The relatively weak value of our ^{1}H MAS NMR chemical shift (4.5 ppm compared to a value of 5.5 ppm in the case of the Vyalikh study[54]) could be explained by the strong confinement in a porous network of diameter of the order of 4 nm, which decreases the average number of hydrogen bonds compared to free water.[55,56]

3.1.3 ^{1}H NMR spectra for samples stored at 30% RH and for baked samples

Similar measurements were performed on samples stored at 30% RH (Figures 2c and 2d), and also on baked samples (spectra not shown here). These last spectra show a significant decrease in the intensity of the signal centred at 4.5 ppm for samples stored at 30% HR, and its disappearance for baked samples. Additional sharp and weak signals were observed at 1 ppm and 0 ppm, which can be attributed to small numbers of hydrogen atoms belonging to hydroxyl groups from silanol and/or Al-OH.[57] Baked samples (at 200 °C for samples previously heat treated at and above 200 °C) showed almost nothing but the fine components from silanols.

Quantitative analyses can be deduced from ^{1}H NMR spectra when the signals come from liquid water. Thus the spectra were calibrated using the rotor signal (the same rotor having been systematically used for each measurement) and quantitative analyses were performed using the data. The 100 % value was attributed to the amount of water in the as-prepared sample stored at 95% RH, and the results are shown in Figure 3a. Variations observed from static and MAS measurements gave similar results. At 95% RH the amount of water is quite unchanged from room temperature up to a heat treatment temperature of 600 °C, and then decreases continuously to reach about 10 weight percent (wt %) at 900 °C and 0 wt % at 1000 °C, indicating the collapse of the porous structure. The water content in the as-prepared sample decreases to about 45 wt % when stored at 30 % RH, and this amount linearly decreases with temperature. Finally, we can note that 200 °C baked samples contained only a few wt % of water, whatever the

temperature of the heat treatment. The FWHM of signals measured from samples stored at 30 % RH, although larger, still decreased with temperature (from FWHM = 9 ppm at room temperature to FWHM = 4 ppm at 600 °C; Figure 3c). At the same time, the chemical shift for these samples was now temperature-dependent, with a decrease in the δ_{iso} value from 4.8 ppm to 4.0 ppm for both the samples stored at 30 % RH and the baked samples (Figure 3b). Similar results have been observed by Vyalikh et al., with a ^{1}H MAS NMR chemical shift decreasing from 5.5 ppm to 3.5 ppm when emptying the water from the porous network of silica glass.[54,58] This decrease in chemical shift is attributed to the fact that free water molecules become hydrogen-bonded to surface hydroxyls.

3.2 DSC analyses

3.2.1 Thermoporosimetry

DSC measurements were performed on samples taken from their wet storage chamber, without adding water. Only the water-filled pores were probed, which can be far from the total porosity of the sample. Several measurements were performed on the as-synthesized sample stored in wet conditions with a relative humidity of between 90% RH and 98% RH (Figure 4a). Three distinct signals were observed; two of them – labelled 1 and 2 in Figure 4 and corresponding to mesoporosity – were not humidity-dependent, whereas a third, temperature-dependent signal (observed for higher crystallization temperatures and labelled 3 in Figure 4) was attributed to incompletely-filled macropores. Analysis of the invariant signals at around -25 °C and -40 °C indicates that they correspond to an apparent pore radius of 2.7 nm and 1.9 nm respectively (Figure 4b). At the same time, comparison with the fusion temperature observed for the third measurement ramp indicated an almost perfect cylindrical feature for the 2.7 nm mesopores (Figure 4c), explaining the large hysteresis observed between fusion and crystallisation signals for confined water.[51] The signal corresponding to the 1.9 nm mesopores was not observed on

the crystallisation ramp. The interpretation of this signal close to -40 °C had already been discussed in the literature, and attributed to water homogenous nucleation, which is observed for cylindrical pores below a critical radius.[59,60]

The variations in DSC signals for thermally treated geopolymer are shown on Figure 5. Both temperature-independent signals (N°1 and 2) evolved only very partially. The signal close to -40 °C split into two components at 200 °C and 300 °C before coming back to a single component up to 800 °C (Figure 5a). The modification of this signal with the temperature of the heat treatment was not in favour of a homogeneous nucleation origin (which excludes any interference from the porous surface); however, the differences observed had no significant repercussions in terms of water containment (the pore radius varying between 1.85 and 2.00 nm; Figure 5b). The second mesopore signal varied between -20 °C and -25 °C, and the corresponding calculated pore radii were a little impacted, with variations between 2.4 nm and 2.9 nm (Figure 5c). And finally, the variation in the third, humidity-dependant signal has no interest here because it corresponds to macroporosity. The collapse of the porous network was evidenced for thermal treatments above 900 °C, then its complete closure above 1000 °C, illustrated by the absence of any signal on the DSC curve, reflecting the impossibility for the heat-treated material to exchange water with the environment.

Measurements performed on samples stored at 30% RH and on samples baked at 200°C demonstrated the absence of free water in the mesopores: the absence of any signal on the DSC curves for all samples from both series (an example from geopolymer heat-treated at 300°C is shown in Figure 5d) indicating the absence, or a very small amount, of water in closed pores.

3.2.2 Thermal weight loss

The airtight aluminum crucibles used for the DSC measurements were then used to quantitatively determine the free water amount contained in the pores as a function of the heat

treatment temperature and the storage conditions. All crucibles were pierced before making fire loss measurements at 400 °C. The water weight amount variations determined in samples stored at 95% RH, at 30% RH and in baked samples were in perfect agreement with the previously-mentioned variations in ^{1}H NMR intensities (Figure 6). To compare both sets of results on the same scale, ^{1}H NMR intensities (from Figure 3a) were normalized by considering the amount of 26 wt % of water for sample 25^{95} (i.e. its determined weight loss). The absence of signal on DSC curves for both the 30% RH and baked series was surely due to the emptying of the mesopores only, with water still present in the macropores for the 30% RH samples. The 200 °C baked samples should be considered as anhydrous, or more precisely as dry. The few weight percent of observed water were certainly only physisorbed water molecules inherent to the manipulations outside the storage chamber required for the preparation of the samples before NMR or DSC experiments.

3.3 Nitrogen adsorption–desorption isotherms

Figure 7 shows nitrogen adsorption–desorption isotherms at 77 K for selected samples. The general shape of the isotherms changed drastically between 800 °C and 900 °C. As-prepared geopolymer (i.e. the measured 25^{30} sample) and samples heat-treated up to 800 °C showed an adsorption isotherm of type IV related to mesoporous materials (according to the IUPAC classification[43]). The renewal of adsorption at capillary condensation (for $P/P_0 > 0.95$), is characteristic of either a combined macroporous network or the presence of an ink-bottle effect in the mesoporous network. During heating, the hysteresis loop changed from type IVb to type IVa, with adsorption and desorption branches that became more and more parallel. The IVb type for the as-prepared geopolymer is certainly due to the presence of ink-bottle mesopores[61] in which desorption is controlled by the narrow necks. Thermal treatments tend to homogenize the cylindrical shape and size of the mesopores.[62,63]

However, this variation in the mesoporous network did not affect the calculated pore radius, which stayed close to ~4 nm (see R_{BJH} in Table 1). On the other hand, the shape of the adsorption branch remained almost unchanged up to 800 °C, with a gentle slope due to capillary condensation into the cylindrical mesoporous channels. Finally, from 900 °C upward, we observed a type III isotherm corresponding to non-porous solids and indicating the complete collapse of the geopolymer porous network.

Table 1 summarizes the main physicochemical parameters of the samples used in the present study and compares results extracted from gas adsorption isotherms, 400 °C weight losses and thermoporismetry. As previously observed for the R_{BJH} average pore size, there is only very little change in the specific surface area up to 800 °C, with a value of around S_{BET} = 80 m^2/g. The only significate variation is observed between the 25^{30} and 100^{30} samples (S_{BET} = 112 m^2/g), with potentially erroneous calculated values for the as-prepared 25^{30} geopolymer due to an incomplete evacuation of water from the porous network. Indeed, in order not to misrepresent the porous characteristics of this untreated sample, degassing was performed at room temperature. Concerning the V_p pore volume (calculated by using the BJH theory, and corresponding to mesopores), we can notice a gradual decrease in the value, from 0.28 cm^3/g for the 25^{30} sample to 0.18 cm^3/g for the 800^{30} sample.

4- Discussion

In this study we focused our investigation on mesopore-type porosity because it is the type that is likely to rehydrate easily by capillary condensation, depending on the surrounding humidity, and therefore likely to provide interest in terms of fire resistance. According to the classification by the International Union of Pure and Applied Chemistry[43] mesoporosity concerns pore widths ranging from 2 nm to 50 nm; with pore widths corresponding to their diameter in the case of

cylindrical pores. Results obtained by thermoporosimetry and nitrogen adsorption – desorption isotherms for our geopolymer (Table 1), in agreement with previously published values, enable us to characterize the geopolymer as a mesoporous material. Furthermore, the observation of our material in different ambient humidity conditions makes it possible to highlight the ability for geopolymers to rehydrate easily.

4.1 Thermal variations in the porous network

The determined physicochemical characteristics of pores having a cylindrical shape, a pore radius of about 5 nm and a specific surface area of around 100 m^2/g agree with previously published characteristics for K-based geopolymers.[36,40] The difference between pore radius values provided by DSC measurements (thermoporosimetry treatment) and nitrogen sorption isotherms, although in a proportion of one to two (Table 1 and Figure 8a), is in fact not aberrant. The strong ink-bottle effect mentioned by Benavant[40] affects the two techniques differently. For DSC measurements, the presence of narrow necks in the mesoporous network separates the zones of water crystallisation, which is no longer continuous. This can also be at the origin of the phenomenon of homogenous nucleation, toward -40 °C, already mentioned in the literature.[59,60] At the same time, such narrow necks impact the hysteresis loop on N_2 adsorption – desorption isotherms, and potentially also affect the renewal of adsorption for $P/P_0 > 0.95$. We have also to indicate that thermoporosimetry was conducted considering water as a probing solvent. It is known that interstitial liquid in geopolymers is far from being pure water, containing in particular large amounts of solvated alkaline cations (potentially 1 mol/L).[64] We have shown that the presence of ions in the solvent (unpublished results using a simulated cementitious interstitial solution for TPM analyses) resulted in a smaller apparent pore radius. It seems, therefore, that the pore size values determined by the BJH method are more accurate. The TPM results remain, however, interesting for the characterization of the morphology of the

mesoporous network, with a clearly marked cylindrical aspect (Figure 4c). Both techniques show a limited variation in the mesoporous characteristics from ambient temperature to 800 °C. We simply note a slight decrease in the apparent porous radius, as well as in the specific surface area (from about 100 m^2/g at room temperature to about 80 m^2/g at 800 °C). By contrast, at a temperature of 900 °C these characteristics change significantly and reflect the collapse of the porous network (with S_{BET} less than 5 m^2/g and the impossibility to evidence porosity) resulting in a condensate ceramic. These findings complete our previously reported results concerning the mineral matrix of this geopolymer, which preserves its intrinsic characteristics up to 900 °C.[30] In the light of these latest results, considering the two porous and mineral sub-networks, we can now say that the geopolymer material is preserved up to a temperature of 800 °C.

The pore volume was determined using three techniques: weight losses at 400 °C on samples hermetically enclosed in DSC crucibles, intensities of the ^1H NMR signal and BJH treatment of the nitrogen adsorption branch. Results from weight losses and ^1H NMR are very close (Figure 6) and illustrate the ability of the geopolymer to rehydrate when stored at 95% RH, even after substantial thermal treatments. The different water amounts determined in samples stored at 30% RH and 95% RH led us to attribute the difference between the two series to capillary condensation, only possible in high humidity conditions. Therefore, the difference between 30% and 95 % RH in Figure 6 corresponds to mesoporosity, and consequently water already present in the samples stored at 30% RH partially fills the macropores. The porous volumes V_p and V_{mes} in Table 1 thus express approximately the same value, corresponding to the mesopore volume. In Figure 8b, their averages were fitted and a constant mesoporous volume of 0.23 cm^3/g emerges from room temperature to 600 °C, followed by a slight drop to 0.17 cm^3/g at 800 °C, before the collapse at 900 °C. Still in Figure 8b, the difference between the merged fitted line for mesopores and the hollow symbols for the total probed pores remains

approximately constant up to 600 °C with a volume of about 0.10 cm^3/g, corresponding to macroporosity.

4.2 Thermal variation in water status

Static and MAS ^1H NMR experiments were carried out in order to discriminate between hydrogen atoms belonging to 'free' liquid water and bonded hydroxyls or water molecules. The comparison of spectra from samples stored at 95% RH (Figures 2a and 2b) simply shows a sharpening of the signal, with the 30 kHz rotor spin indicating that the vast majority of the protons present in the geopolymer correspond to liquid water molecules filling the porous network. Again, the intensity of the signals from the heat-treated samples shows the ability of the material to rehydrate when stored in a humid atmosphere, and therefore illustrates the fact that the porous network is open and traversing. Figure 3a highlights that this is particularly true up to a temperature of 700 °C. At 800 °C the signal intensity is approximately halved, then almost nonexistent beyond this temperature, in agreement with previous results on pore volume determination and its variation with temperature. Spectra recorded for samples stored at 30% RH complete these observations (Figure 2c and 2d) with additional signals (close to 0 ppm) of low intensity in MAS spectra. These additional signals, related to non-mobile hydrogen atoms, were attributed to silanol Si–OH (or aluminol Al–OH) entities present in limited quantity. The low number of –OH entities in the geopolymer agrees with the TGA curve,[30] showing a weak dehydroxylation around 400 °C. In addition to the sharpening of the signal with magic angle spinning, there is also a sharpening associated with the temperature of the heat treatment for both series: FWHM varies from 5.5 to 2.5 ppm for the static series and from 4 to 1 ppm for the MAS series (Figure 3c). Moreover, we can observe that this FWHM sharpening is performed without any variation in the isotropic chemical shift when the material is saturated with water (figure 3b). This allows us to conclude that the status of the water has not changed as a result

of heat treatments. In high humidity, we are always in the presence of liquid water which fills the pores. It appears more and more 'free' during the increase in temperature, which can be explained either by a decrease in its confinement (i.e. an increase in the size of the mesopore), or by a decrease in its salinity (i.e. a decrease in its alkalinity). Findings from the previous paragraph indicate a minimal variation in mesopore size, which would not explain a variation in the FWHM. On the other hand, a reduction in interstitial water alkalinity would mean that following the heat treatments the pore-filling liquid would be increasingly pure water. This is then in agreement with the observations made on the variations in the mineral matrix in the previous study,[30] which concluded that the potassium cations in the pore solution pass through the mineral sub-network during the rise in temperature. There would be a variation in the pore surface chemistry that could explain the variation in the chemical shift for the 30% RH and baked series. For the samples from these two series the pores are not filled; water molecules are physisorbed to the porous interface, which evolves with the fixation of potassium. This non-liquid water status explains the absence of a DSC signal for these two series of samples (Figure 5d).

5- Conclusion

The combination of several complementary techniques for the characterisation of the porous network (^{1}H static and MAS NMR, DSC with TPM treatment, thermal weight loss, nitrogen adsorption–desorption isotherms) led to a precise description of the mesoporosity of a geopolymer. The porosity of our investigated K-based geopolymer agrees very well with the porous structure of metakaolin-based geopolymers detailed by Benavent,[40] including the strong 'ink-bottle' effect due to a two-level pore structure composed of interlinked meso- and macroporous networks. Almost the entire porous network is accessible to water, thus translating

the fact that the closed pore volume is very low. Water from the porous network can easily and without damage leave the geopolymer during a rise in temperature. This water flow is totally reversible (for heat treatments up to 700 °C) in the presence of significant relative humidity. For heat treatment at 800 °C, half of the pore volume has disappeared, and at 900 °C the material is no longer porous. By combining the results from parts 1 and 2 on the temperature stability of our K-based geopolymer we can confirm, without any ambiguity, that the geopolymer retains its whole mineral and porous characteristics up to a temperature of 700 °C. At 800 °C we are still in the presence of a geopolymer-type material, with half the original pore volume. At 900 °C the mineral network is still amorphous with a 3D connection of the aluminate and silicate tetrahedra, but with the disappearance of the porous nature specificity of geopolymers which is becoming a dense ceramic. Finally, at 1000 °C, there is the beginning of crystallization, and the disappearance of any characteristics of a geopolymer.

Thus it can be concluded that a high-temperature application (refractory, up to 700-800 °C for a potassium geopolymer) is absolutely conceivable. Furthermore, the rehydration ability of the material gives it interesting fireproof properties, with about 25 weight percent of easily available liquid water.

Acknowledgements

Project supported by Andra under the "Investing in the Future" Programme ("Investissement d'Avenir") - Selected under the Andra Call for Projects: "Optimisation of post-dismantling radioactive waste management", organised in cooperation with the French National Research Agency (ANR).

References

[1] Provis JL, Van Deventer JSJ. Geopolymers: Structures, Processing, Properties and Industrial Applications. Woodhead Publishing, Abingdon UK; 2009.

[2] Provis JL, Duxson P, van Demeter JSJ, Lukey GC. The role of mathematical modelling and gel chemistry in advancing geopolymer technology. Chem. Eng. Res. Des. 2005; 83: 853–860.

[3] Duxson P, Fernández-Jiménez A, Provis JL, Lukey GC, Palomo A, van Demeter JSJ. Geopolymer technology: the current state of the art. J. Mater. Sci. 2007; 42: 2917–2933.

[4] Chlique C, Lambertin D, Antonucci P, Frizon F, Deniard P. XRD analysis of the role of cesium in sodium-based geopolymer. J. Am. Ceram. Soc. 2015; 98: 1308–1313.

[5] Kriven WM, Bell JL, Gordon M. Microstructure and nanoporosity of as-set geopolymers. Ceram. Eng. Sci. Proc. 2007; 27: 491–503.

[6] Kong DLY, Sanjayan JG, Sagoe-Crentsil K. Comparative performance of geopolymers made with metakaolin and fly ash after exposure to elevated temperatures. Cem. Concr. Res. 2007; 37: 1583–1589.

[7] Li Z, Chen R, Zhang LY. Utilization of chitosan biopolymer to enhance fly ash-based geopolymer. J. Mater. Sci. 2013; 48: 7986–7993.

[8] Palomo A, Blanco-Valera MT, Granizo ML, Puertas F,Vazquez T, Grutzeck MW. Chemical stability of cementitious materials based on metakaolin. Cem. Concr. Res. 1999; 29: 997–1004.

[9] Babushkin V, Matveyev G, Mchedlov-Petrossyan O. Thermodynamics of Silicates. Springer-Verlag, Berlin; 1985.

[10] Xu H, Van Deventer JSJ. The geopolymerisation of alumino-silicate minerals. Inter. J. Mine. Process.2000; 59: 247–266.

[11] Dimas D, Giannopoulou I, Panias D. Polymerization in sodium silicate solutions: a fundamental process in geopolymerization technology. J. Mater. Sci. 2009; 44: 3719–3730.

[12] Duxson P, Provis JL, Lukey GC, van Demeter JSJ. The role of inorganic polymer technology in the development of 'green concrete. Cem. Concr. Res. 2007; 37: 1590–1597.

[13] Weil M, Dombrowski K, Buchwald A. Life-cycle analysis of geopolymers in geopolymers. Woodhead Publishing, Abingdon UK. 2009; p. 194–210.

[14] McLellan BC, Williams RP, Lay J, van Riessen A, Corder GD. Costs and carbon emissions for geopolymer pastes in comparison to ordinary portland cement. J. Clean. Prod. 2011; 19: 1080–1090.

[15] Habert G, Ouellet-Plamondon C. Recent Update on the Environmental Impact of Geopolymers. RILEM Technical Letters. 2016; 1: 17–23.

[16] Pacheco-Torgal F, Abdollahnejad Z, Camões AF, Jamshidi M, Ding Y. Durability of alkali-activated binders: a clear advantage over portland cement or an unproven issue? Constr. Build. Mater. 2012; 30: 400–405.

[17] Barbosa VFF, macKenzie KJD. Thermal behaviour of inorganic geopolymers and composites derived from sodium polysialate. Mater. Res. Bull. 2033; 38: 319–331.

[18] Fernández-Jiménez A, Palomo A, Pastor JY, Martin A. New cementitious materials based on alkali activated fly ash: performance at high temperatures. J. Am. Ceram. Soc. 2008; 91: 3308–3314.

[19] Malviya M, Goliya H. Durability of fly ash based geopolymer concrete using alkaline solutions (NaOH and Na_2SiO_3). Int. J. Emerg. Tre. Eng. Dev. 2014; 6: 18–33.

[20] Pacheco-Torgal F, Castro-Gomes JP, Jalali S. Bond strength between concrete substance and repair materials: comparisons between tungsten mine waste geopolymeric binder versus current commercial repair products. 7th International Congress on Advances in Civil Engineering, Istanbul Turkey; 2006.

[21] Palomo A, Lopez de la Fuente JI. Alkali-activated cementitous materials: Alternative matrices for the immobilisation of hazardous wastes: Part I. Stabilisation of boron. Cem. Concr. Res. 2003; 33: 281–288.

[22] Lambertin D, Frizon F, Blachere A, Bart F. Corrosion behaviour of Mg alloys in various basic media: Application of waste encapsulation of fuel decanning from UNGG nuclear reactor. in Magnesium Technology, John Wiley & Sons Inc. 2011; p. 435–439.

[23] Cantarel V, Nouaille F, Rooses A, Lambertin D, Poulesquen A, Frizon F. Solidification/stabilisation of liquid oil waste in metakaolin-based geopolymer. J. Nucl. Mater. 2015; 464: 16–19.

[24] Duxson P, Lukey GC, van Deventer JSJ. Evolution of gel structure during thermal processing of Na-geopolymer gels. Langmuir. 2006; 22: 8750–8757.

[25] Duxson P, Lukey GC, van Deventer JSJ. Physical evolution of Na-geopolymer derived from metakaolin up to 1000 °C. J. Mater. Sci. 2007; 42: 3044–3054.

[26] Rahier H, Wastiels J, Biesemans M, Willem R, van Asshe G, van Mele B. Reaction mechanism, kinetics and high temperature transformation of geoplymers. J. Mater. Sci. 2007; 42: 2982-2996.

[27] Buchwald A, Vicent M, Kriegel R, Kaps C, Monzó M, Barba A. Geopolymeric binders with different fine fillers — Phase transformations at high temperatures. Appl. Clay Sci. 2009; 46: 190–195.

[28] Barbosa VFF, macKenzie KJD. Synthesis and thermal behaviour of potassium sialate geopolymers. Mater. Lett. 2003; 57: 1477–1482.

[29] Tchakouté HK, Rüscher CH, Kong S, Kamseu E, Leonelli C. Thermal behavior of metakaolin-based geopolymer cements using sodium waterglass from rice husk ash and waste glass as alternative activators. Waste and Biomass Valorization. 2017; 8: 573-584.

[30] Gomes S, Petit E, Frezet L, Thirouard R, Taviot-Gueho C, Gharzouni A, et al. Temperature stability of a pure metakaolin based K-geopolymer: Part 1. Variations in the amorphous mineral network. J. Amer. Ceram. Soc. 2020; *to be publish*.

[31] Jämstorp E, Strømme M, Frenning G. Modeling structure–function relationships for diffusive drug transport in inert porous geopolymer matrices. J. Pharma. Sci. 2011; 100: 4338-4348.

[32] Boher C, Martin I, Lorente S, Frizon F. Experimental investigation of gas diffusion through monomodal materials. Application to geopolymers and Vycor® glasses. Micropor. Mesopor. Mater. 2014; 184: 28-36.

[33] Maitland CF, Buckley CE, O'Connor B, Butler PD, Hard RD. Characterization of the pore structure of metakaolin-derived geopolymers by neutron scattering and electron microscopy. J. Appl. Cryst. 2011; 44: 697-707.

[34] Metroke TL, Henley MV, Hammons MI. Effect of curing conditions on the porosity characteristics of metakaolin–fly ash geopolymers, in Strategic Materials and Computational Design., John Wiley & Sons, Inc. 2010; p. 11-15.

[35] Sindhunata, Provis JL, Luckey GC, Xu H, van Deventer JSJ. Structural evolution of fly ash based geopolymers in alkaline environments," Indus. Engin. Chem. Res. 2008; 47: 2991-2999.

[36] Kriven W, Gordon M, Bell J. Geopolymers: nanoparticulate, nanoporous ceramics made under ambient conditions. Microsc. Microanal. 20045; 10: 404-405.

[37] Duxson P, Provis JL, Lukey GC, Mallicoat SW, Kriven WM, van Deventer JSJ. Understanding the relationship between geopolymer composition, microstructure and mechanical properties. Colloids Surf. A: Physicochem. Engin. Aspects. 2005; 269: 47-58.

[38] Lloyd RR, Provis JL, Smeaton KJ, van Deventer JSJ. Spatial distribution of pores in fly ash-based inorganic polymer gels visualised by Wood's metal intrusion. Micropor. Mesopor. Mater. 2009; 126: 32-39.

[39] Provis JL, Myers RJ, White CE, Rose V, van Deventer JSJ. X-ray microtomography shows pore structure and tortuosity in alkali-activated binders. Cem. Concr. Res. 2012; 42: 855-864.

[40] Benavent V, Frizon F, Poulesquen A. Effect of composition and aging on the porous structure of metakaolin-based geopolymers. J. Appl. Cryst. 2016; 49: 2116-2128.

[41] Melar J, Renaudin G, Leroux F, Hardy-Dessource A, Nedelec JM, Taviot-Gueho C, et al. The porous network and its interface inside geopolymers as a function of alkali cation and aging. J. Phys. Chem. C. 2015; 119: 17619-17632.

[42] Brun M, Lallemand A, Quinson JF, Eyraud C. A new method for the simultaneous determination of the size and shape of pores: the thermoporometry. Thermochim. Acta. 1977; 21: 59–88.

[43] Rouquerol J, Avnir D, Fairbridge CW, Everett DH, Haynes JM, Pernicone N, et al. Recommendations for the characterization of porous solids (Technical Report). Pure Appl. Chem. 1994; 66: 1739-1758.

[44] Brunauer S, Emmett PH, Teller E. Adsorption of gases in multimolecular layers. J. Amer. Chem. Soc. 1938; 60: 309–319.

[45] Bellissent-Funel MC, Chen SH, Zanotti JM. Single-particle dynamics of water molecules in confined space. Phys. Rev. E. 1995; 51: 4558-4569.

[46] Floquet N, Coulomb JP, Dufau N, Andre G, Kahn R. Structural and dynamic properties of confined water in nanometric model porous materials (8 Å $\leq \varnothing \leq$ 40 Å). Physica B Cond. Mat. 2004; 350: 265-269.

[47] Takahara S, Kittaka S, Mori T, Kuroda Y, Yamaguchi T, Bellisent-Funel MC. Neutron scattering study on dynamics of water molecules confined in MCM-41. Adsorption. 2005; 11: 479-483.

[48] Takahara S, Sumiyama N, Kittaka S. Neutron scattering study on dynamics of water molecules in MCM-41.2. Determination of translational diffusion coefficient. J. Phys. Chem. B. 2005; 109: 11231-11239.

[49] Mitra S, Mukhopadhyay R, Tsukushi I, Ikeda S. Dynamics of water in confined space (porous alumina): QENS study. J. Phys.: Cond. Mat. 2001; 13: 8455-8465.

[50] Shen H, Maekawa H, Kawamura J, Matsumoto Y, Yamamura T, Kawakita Yet al. Effect of pore size and salt doping on the protonic conductivity of mesoporous alumina. Sol. Sta. Ionics. 2008; 179: 1133-1137.

[51] Briman IM, Rebiscoul D, Diat O, Zanotti JM, Jollivet P, Barboux P, et al. Impact of pore size and pore surface composition on the Dynamics of confined water in highly ordered porous silica. J. Phys. Chem. C. 2012; 116: 7021-7028.

[52] Mamontov E, Cole DR. Quasielastic neutron scattering study of dynamics of $CaCl_2$ aqueous solution confined in Vycor glass. Phys. Chem. Chem. Phys. 2006; 8: 4908-4914.

[53] Mamontov E, Cole DR, Dai S, Pawel MD, Liang CD, Jenkins T, et al. Dynamics of water in LiCl and $CaCl_2$ aqueous solutions confined in silica matrices: A backscattering neutron spectroscopy study. Chem. Phys. 2008; 352: 117-124.

[54] Vyalikh A, Emmler T, Grüberg B, Xu Y, Shenderovich I, Findenegg GH, et al. Hydrogen bonding of water confined in controlled-pore glass 10-75 studied by ^{1}H-solid state NMR. Zeit. Phys. Chem. 2007; 221: 155-168.

[55] Hartnig C, Witschel W, Spohr E, Gallo P, Ricci MA, Rovere M. Modification of the hydrogen bond network of liquid water in a cylindrical SiO_2 pore. J. Mol. Liq. 2000; 85: 127-137.

[56] Thompson H, Soper AK, Ricci MA, Bruni F, Skipper T. The three-dimensional structure of water confined in nanoporous Vycor glass. J. Phys. Chem. B. 2007; 111: 5610-5620.

[57] Stepanov AG. Chapter 4 – Basics of solid-state NMR for application in zeolite science: material and reaction characterization, in Zeolites and zeolite-like materials, edited by Bert Sels, Lesnig Kustov, publisher: Elsevier. 2016; 4: p. 137-188.

[58] Grünberg B, Emmler T, Gedat E, shenderovich I, findenegg GH, Limbach HH, et al. Hydrogen bonding of water confined in mesoporous silica MCM-41 and SBA-15 studied by ^{1}H solid-state NMR. Chem. Europ. J. 2004; 10: 5689-5696.

[59] Morishige K, Yasunaga H, Denoyel R, Wernert V. Pore-blocking-controlled freezing of water in cagelike pores of KIT-5. J. Phys. Chem. C. 2007; 111: 9488-9495.

[60] Khokhlov A, Valiullin R, Kärger J, Steinbach F, Feldhoff A. Freezing and melting transitions of liquids in mesopores with ink-bottle geometry. New J. Phys. 2007; 9: 272-280.

[61] Sing KSW, Everett DH, Haul RAW, Moscou L, Pierotti RA, Rouquerol J, et al. Reporting physisorption data for solid/gas systems, in Handbook of Heterogeneous Catalysis, eds G. Ertl, H. Knözinger, F. Schüth and J. Weitkamp, Wiley-VCH Verlag GmbH and Co; 2008.

[62] Huo Q, Margolese DI, Stucky GD. Surfactant control of phases in the synthesis of mesoporous silica-based materials. Chem. Mat. 1996; 8: 1147-1160.

[63] Kruk M, Jaroniec M, Sayari A. Application of large pore MCM-41 molecular sieves to improve pore size analysis using nitrogen adsorption measurements. Langmuir. 1997; 13: 6267-6273.

[64] Lloyd RR, Provis JL, van Deventer JSJ. Pore solution composition and alkali diffusion in inorganic polymer cement. Cem. Concr. Res. 2010; 40: 1386-1392.

Figures

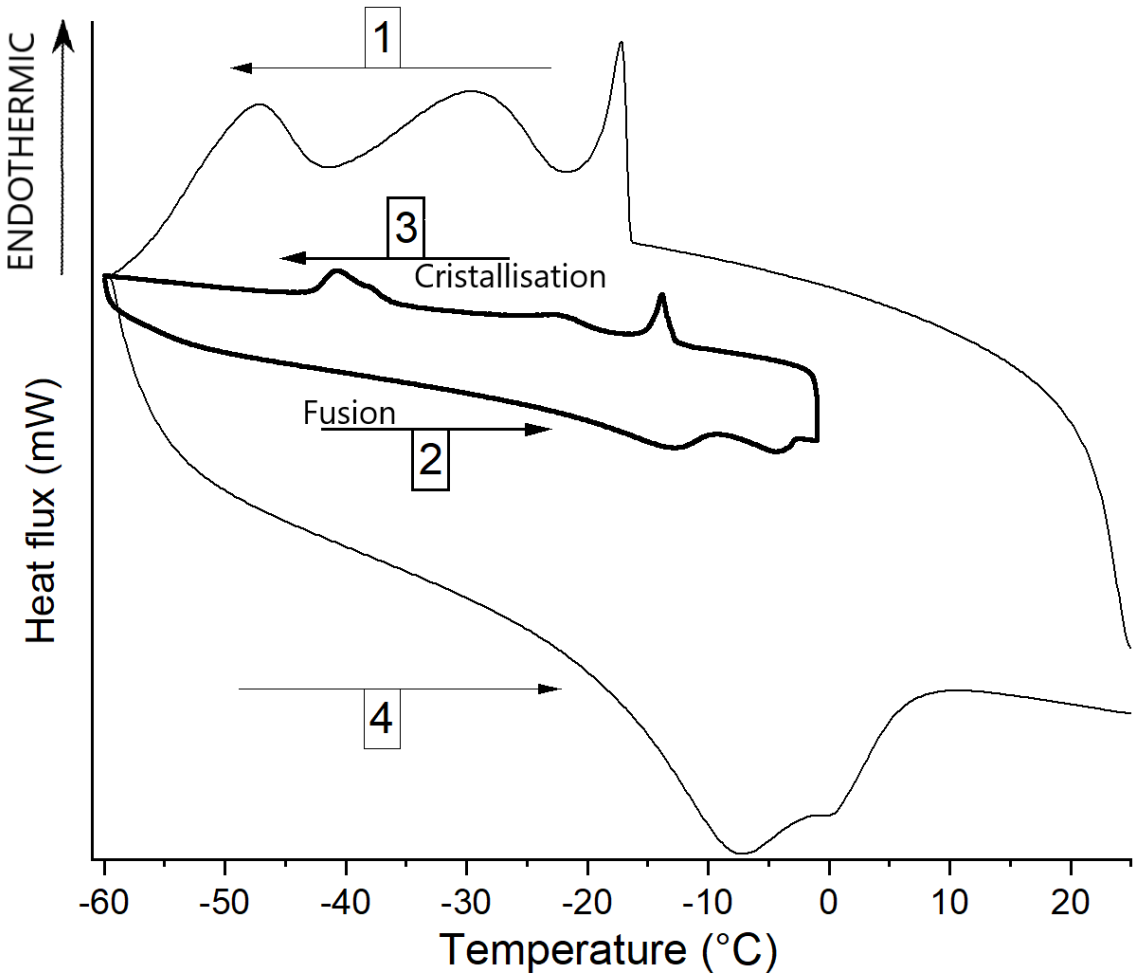

Figure 1. The four steps of the thermoporosimetry method (segments 2 and 3 only were used for data processing).

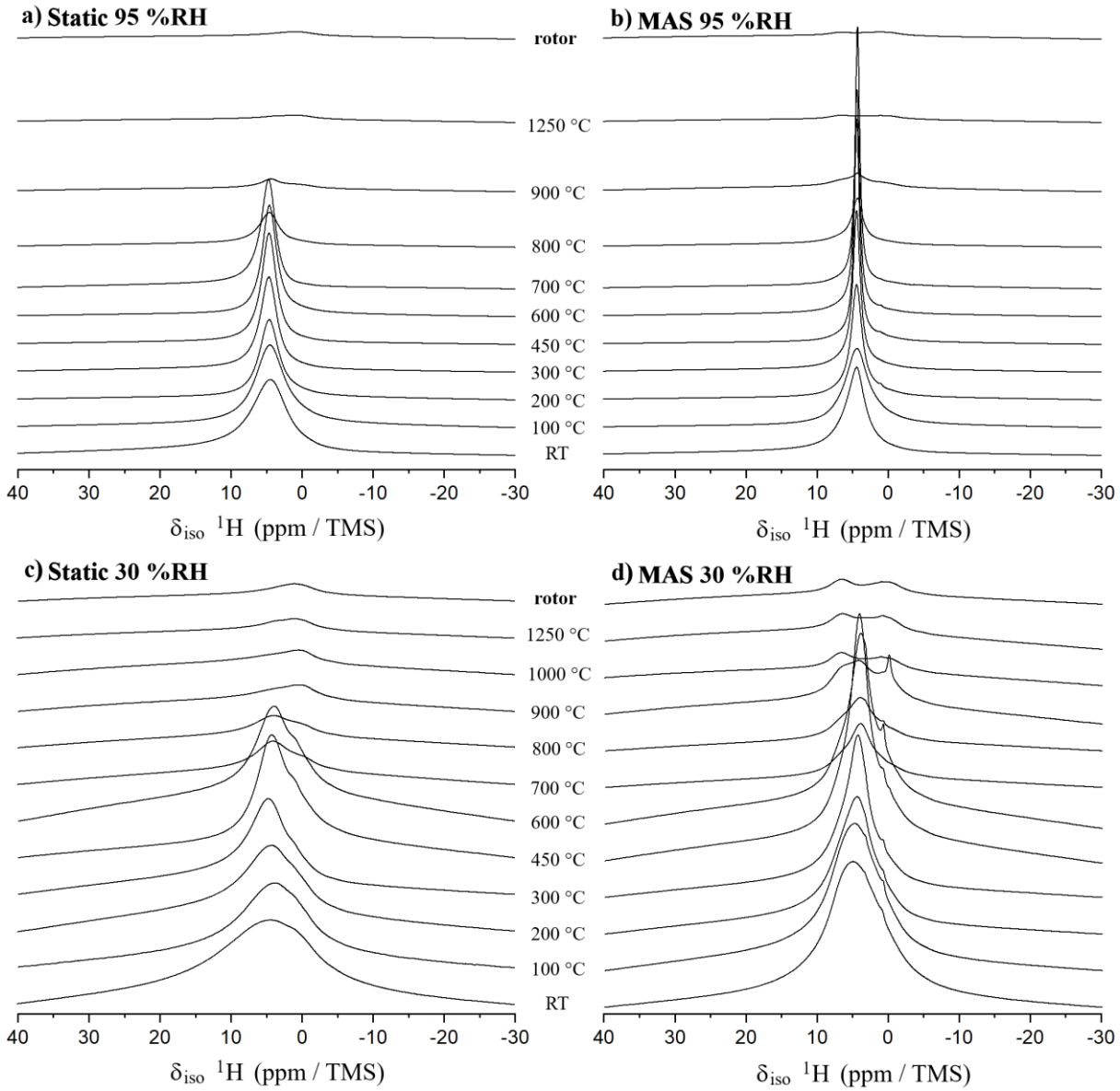

Figure 2. ^{1}H NMR measurements – static (a and c) and MAS (b and d) – for heat-treated geopolymers stored at 95 % RH (a and b) and 30 % RH (c and d).

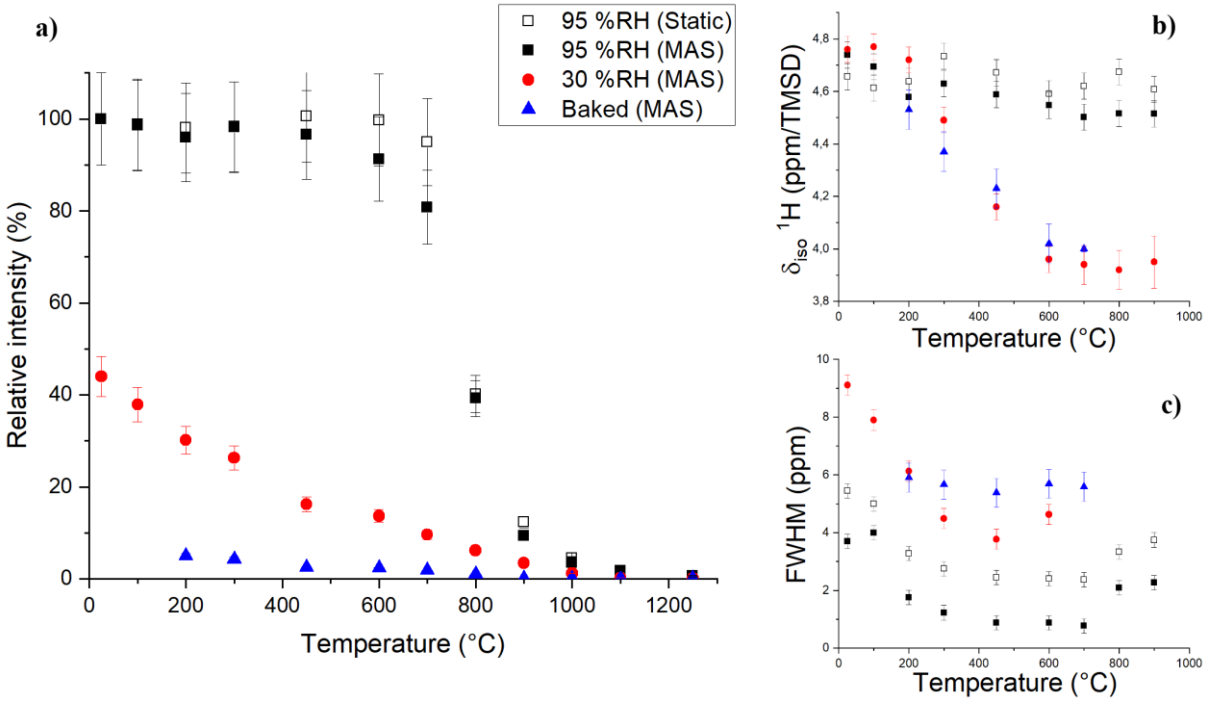

Figure 3. Results from the Lorentzian modeling of the ^{1}H NMR spectra (a: signal intensities, b: chemical shift, and c: Full Width at Half Maximum signal).

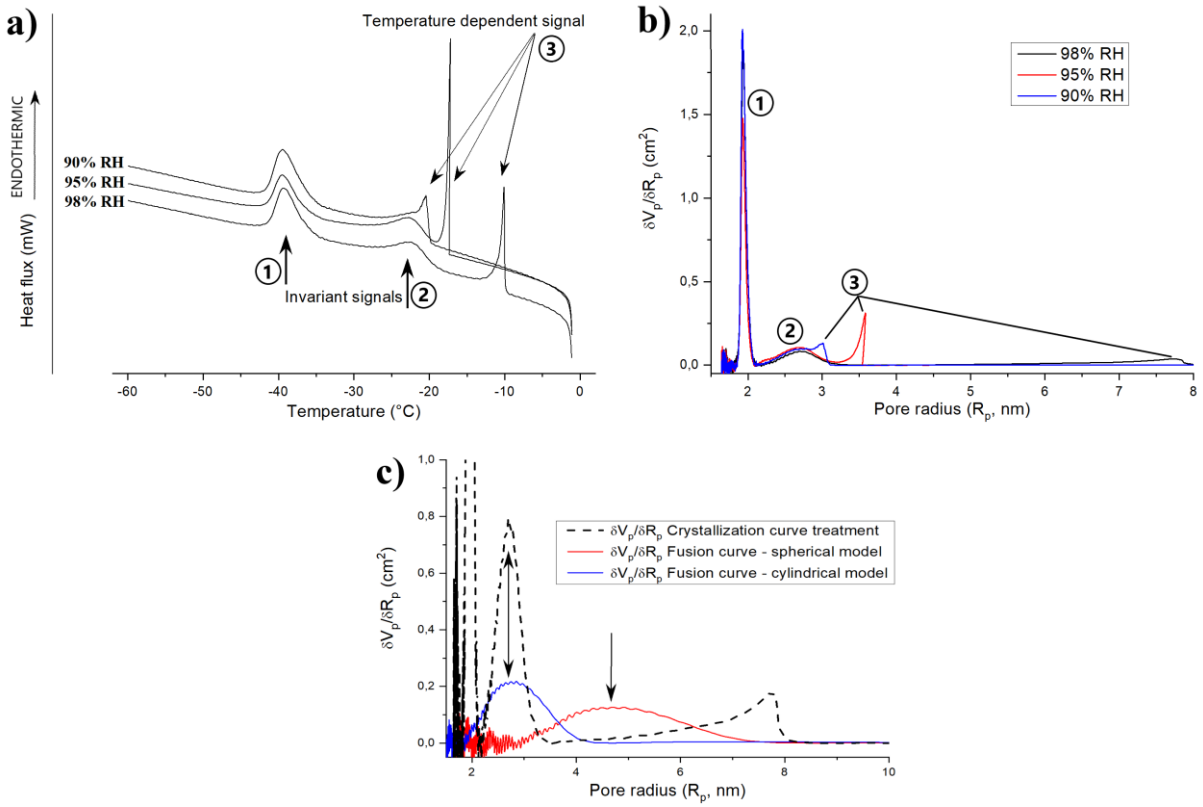

Figure 4. Thermoporosimetry realized on the as-synthesized geopolymer – without heat treatment – taken from three high relative humidity storage conditions (90%, 95% and 98% RH): a. the third crystalizing measured ramp, b. corresponding analytical treatments of these crystalizing measurements, c. comparison with the analytical treatments of the second fusion ramp for the 98% RH sample.

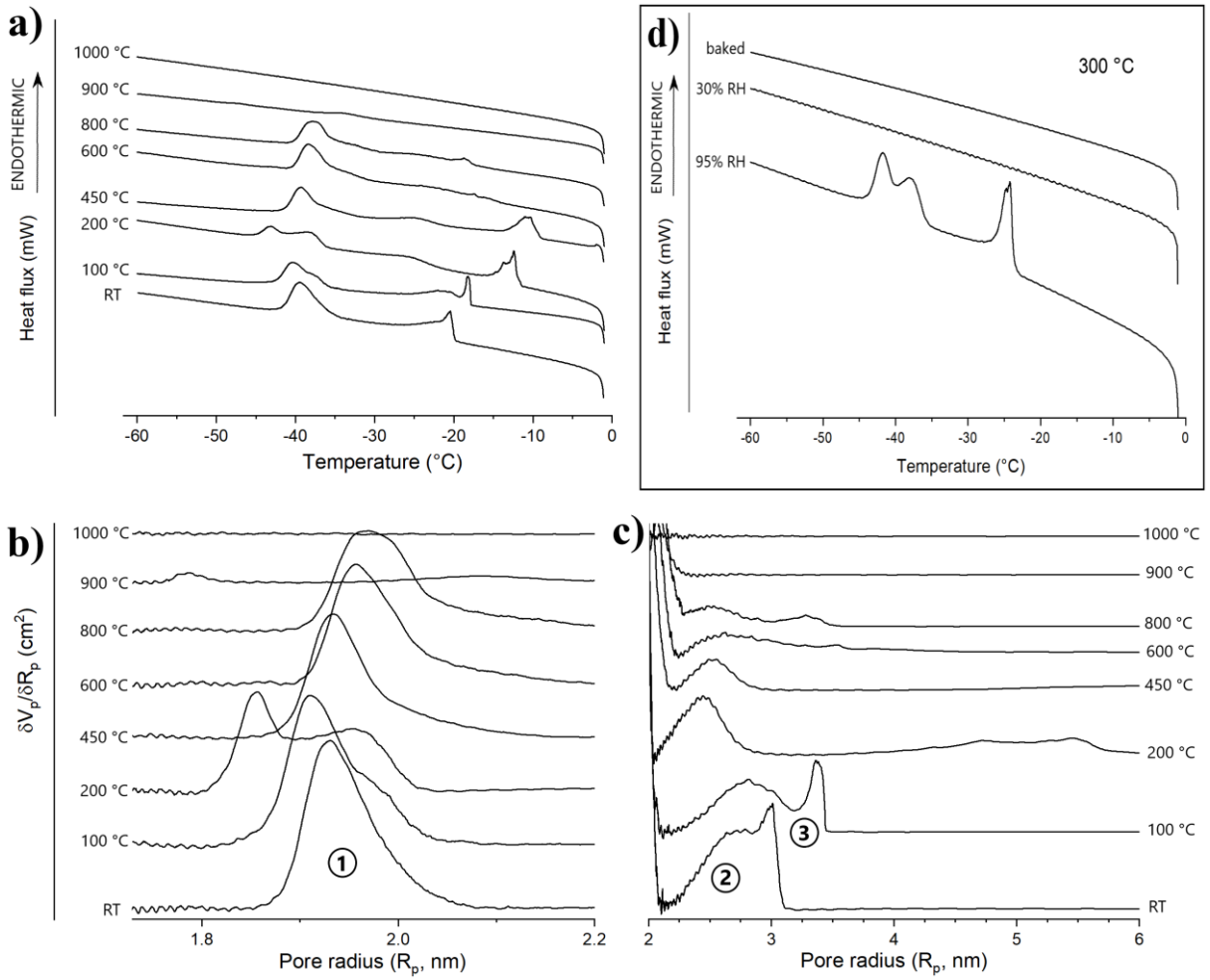

Figure 5. Thermoporosimetry performed on the heat-treated geopolymers: a. the third crystalizing measured ramp from samples stored at 95% HR, b. corresponding analytical treatments for signal N°1, c. corresponding analytical treatments for signal N°2, the third crystalizing measured ramp from the samples heat treated at 300 °C for the three storing conditions (95% RH, 30% RH and baked).

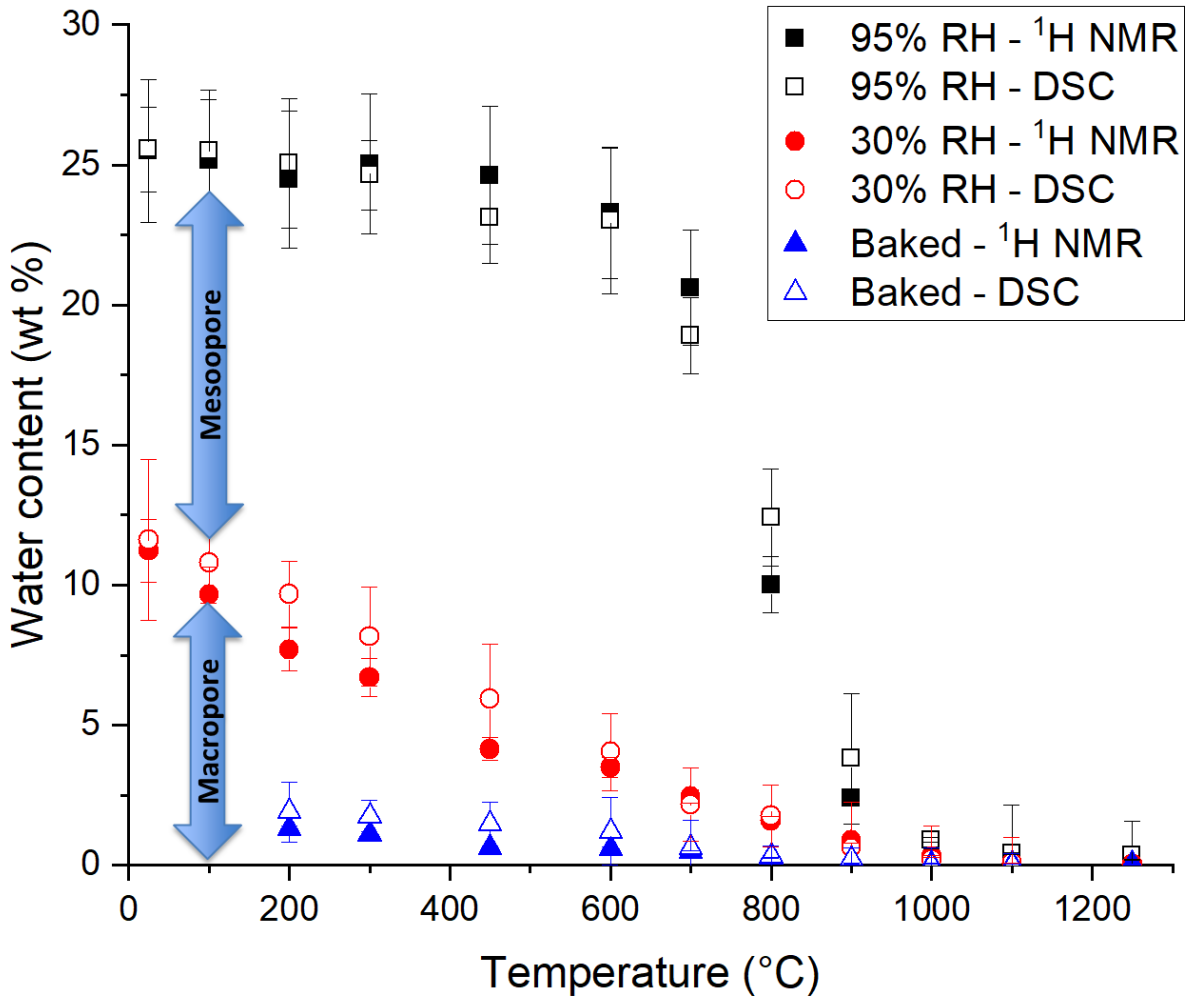

Figure 6. Water amount quantification determined by weight losses at 400 °C (hollow symbols, labeled DSC in the key) and comparison with the variations previously observed by ^{1}H NMR measurements (solid symbols, normalized by considering the amount of 26 wt % water for sample 25[95]).

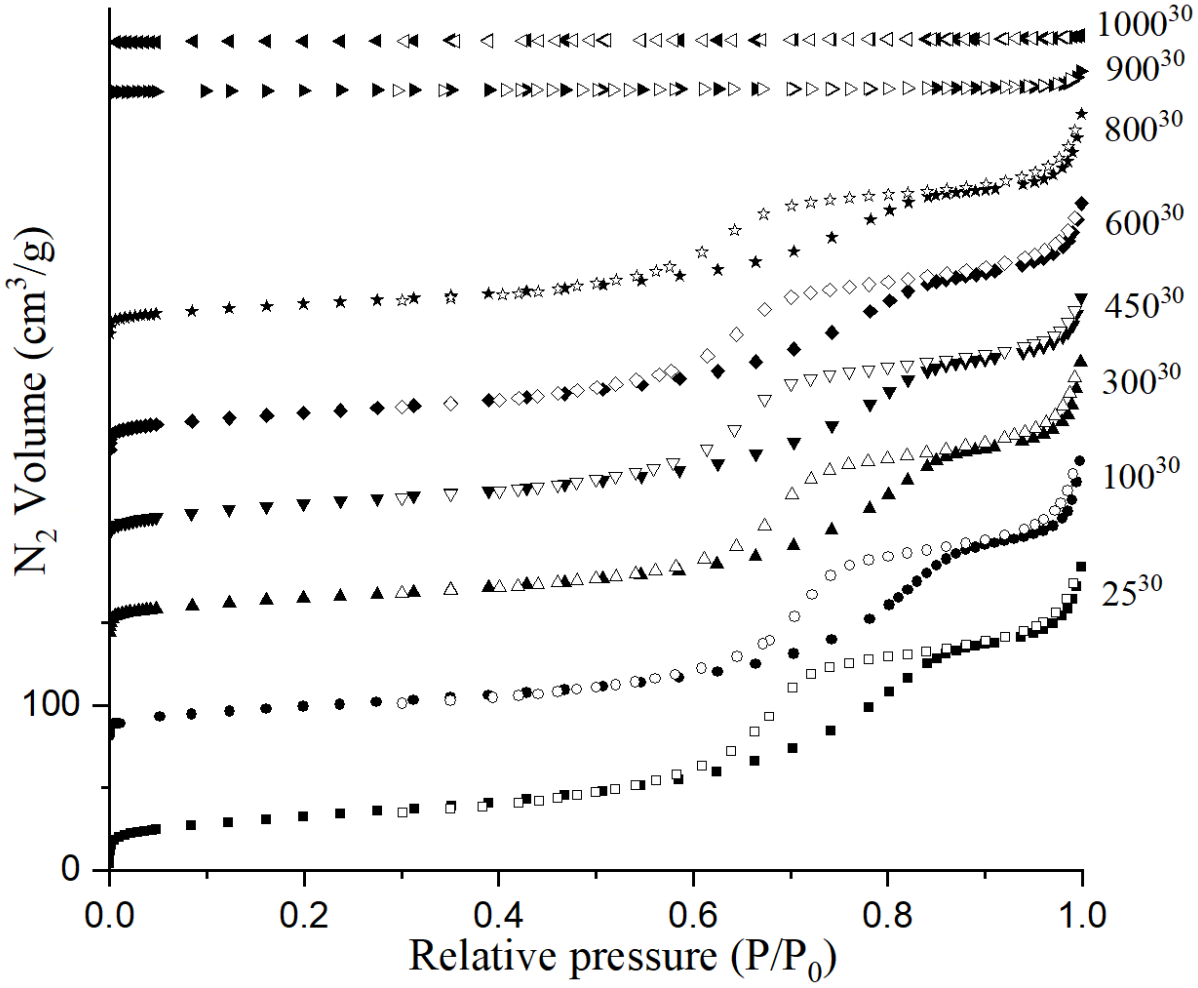

Figure 7. Adsorption – desorption isotherms of nitrogen at 77 K for heat-treated geopolymers. Hollow and solid symbols denote adsorption and desorption points, respectively.

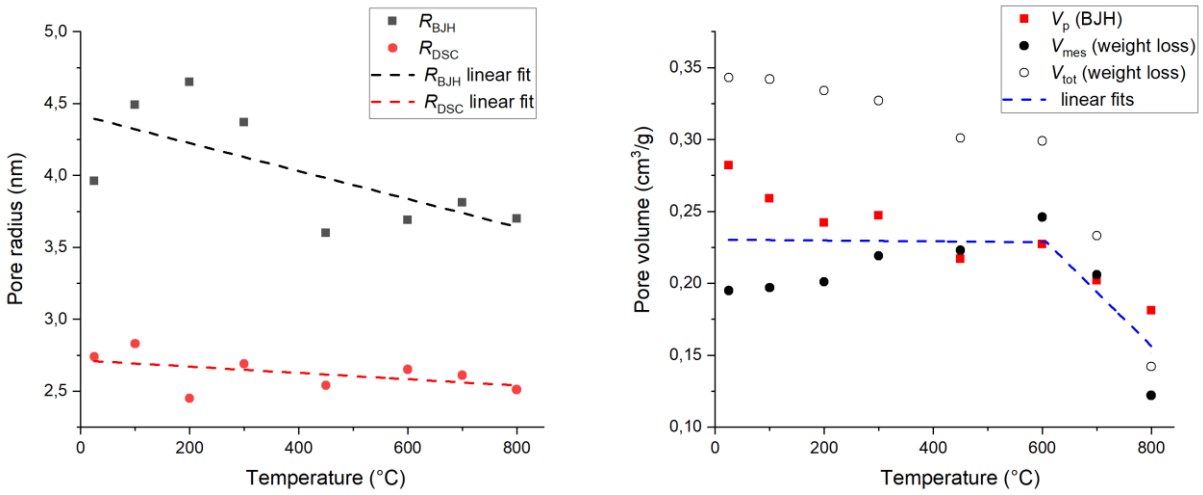

Figure 8. Physicochemical characteristics of the mesoporous network determined using several techniques. a: pore radius (measurements and linear fits), b: pore volume (measurements and linear fit on averaged mesoporous part).